

## Computational fluid dynamics-based design of anoxic bioreactor zone in wastewater treatment plant

Islam Amin<sup>a,b</sup>, Mohamed Elsakka<sup>c</sup>, Selda Oterkus<sup>b,\*</sup>, Cong Tien Nguyen<sup>b</sup>, Murat Ozdemir<sup>b</sup>, Abdel-Hameed El-Aassar<sup>d</sup>, Hosam Shawky<sup>d</sup>, Erkan Oterkus<sup>b</sup>

<sup>a</sup>Department of Naval Architecture and Marine Engineering, Port Said University, Port Said, Egypt, email: i.amin@strath.ac.uk (I. Amin)

<sup>b</sup>Naval Architecture, Ocean and Marine Engineering, University of Strathclyde, Glasgow, UK, emails: selda.oterkus@strath.ac.uk (S. Oterkus), nguyen-tien-cong@strath.ac.uk (C.T. Nguyen), murat.ozdemir@strath.ac.uk (M. Ozdemir), erkan.oterkus@strath.ac.uk (E. Oterkus)

<sup>c</sup>Mechanical Power Engineering Department, Port Said University, Port Said, Egypt, email: elsakka@eng.psu.edu.eg (M. Elsakka)

<sup>d</sup>Egyptian Desalination Research Center (EDRC), Desert Research Center (DRC), Cairo, Egypt, emails: hameed\_m50@yahoo.com (A.-H. El-Aassar), shawkydrc@hotmail.com (H. Shawky)

Received 6 June 2021; Accepted 9 February 2022

### ABSTRACT

Hydrodynamics-based design of an anoxic bioreactor tank is one of the serious challenges in wastewater industry. Poor fluid flow may cause settlement and therefore reduce the biological performance of a bioreactor. Whilst, a successful bioreactor design can facilitate the enhancement of biological process efficiency and reduction of energy consumption so that the investment and operation cost can be kept as low as possible. In the present study, three-dimensional computational fluid dynamics models for three common full-scale bioreactor configurations were simulated using a single-phase flow model and the standard two-equation SST  $k-\epsilon$  turbulence model. The main objective of this numerical study is to investigate the effect of bioreactor geometry on the hydrodynamics performance of the flow field. Four submerged impellers were modelled for each tank geometry and three thrust scenarios were considered in order to evaluate the effect of changing impeller thrust on the flow velocity distribution inside each tank. The results show that the orbital bioreactor geometry has better performance in driving the flow field with more uniform flow patterns than other bioreactor configurations. The minimum flow velocity required was achieved in orbital tank to maintain the micro-organism particles suspended in the wastewater media at certain mixing power.

**Keywords:** Computational fluid dynamics; Design of bioreactor tank; Hydrodynamics based design; Oxidation tank; Rectangular tank; Circular tank

### 1. Introduction

Nowadays, wastewater treatment is one of the important topics to ensure adequate and clean water supply for populations which suffer from water scarcity problems. United Nations (UN) aims to ensure availability and sustainability management of water by encouraging water treatment

programmes. The core and fundamental component of wastewater treatment plants (WWTPs) is biological wastewater treatment, which is used to extract biodegradable organic waste and suspended solid from raw wastewater [1]. Regarding energy consumption, bioreactor zones can consume up to 70% of the overall energy needed for the whole treatment process [2].

\* Corresponding author.

Most large WWTPs remove carbon, nutrients and phosphorus from wastewater by using bioreactor zones. Although there are different operational parameters that affect the efficiency of bioreactors such as detention time, suspended solids concentration, internal recycle rate influent biological oxygen demand (BOD) and biodegradable chemical oxygen demand (COD), the direct bioreactor design parameter that is affected by the hydrodynamics is the detention time which is directly impacted by the anoxic tank configuration [3]. Since the wastewater treatment efficiency depends on the flow field in the bioreactor, a clear understanding of bioreactor hydrodynamic behaviour is needed for an efficient design [4]. Furthermore, due to treatment process complexity, the hydraulics of the bioreactor is often not sufficient tool. Therefore, there is a need for a hydrodynamic-based design that takes into account the geometry of the bioreactor tank which can improve treatment efficiency to meet effluent quality requirements.

Wastewater treatment process faces numerous problems due to poorly designed influent bioreactors that resulted in a significant mal-distribution of flow. Wide inequalities of distribution are often revealed through visual examination, float testing and tracer testing approaches [5]. With the improvement of computational fluid dynamics (CFD), the numerical modelling is a valuable tool used by many researchers to predict and evaluate the effect of hydrodynamic behaviour on the bioreactor performance. For example, flow pattern in oxidation ditch bioreactor has been studied by using a three-dimensional model [6]. The mixing process was obtained by the utilization of the Navier–Stokes equation [7]. Simulation of flow in an oxidation ditch bioreactor driven by mechanical surface aerator was performed using CFD [8]. Yong et al. [9] proposed an integral energy model to optimize the surface aeration control in oxidation ditches using CFD model in their study. Their control system achieved 10% saving in energy consumption. Several techniques are used to model the hydrodynamics and the residence time distribution in an oxidation ditch using Reynolds averaged Navier–Stokes simulations (RANS) and unsteady RANS with the standard  $k-\epsilon$  model, and large eddy simulation with the Smagorinsky subgrid-scale model [10]. In a full-scale oxidation ditch, single-phase CFD models were used to investigate the fluid behaviour using velocity profiles and the aeration patterns [11]. In their comprehensive review of CFD investigations of water treatment units, Rosa et al. [12] concluded that the SST  $k-\epsilon$  and Reynolds Stress Model provide better results in contrast with the other simpler models. Furthermore, several researchers successfully utilized the SST  $k-\epsilon$  model in the simulation of full-scale ditch [11,13].

The orbal bioreactor is a modification of oxidation ditch which is equipped with mechanical mixing devices. The flow velocity in the outer channel of an orbal oxidation bioreactor in a full-scale wastewater treatment plant in China was simulated and monitored under actual operational conditions [14]. Rehman et al. [15], presented a numerical study to visualize the local impacts of flow mixing by proposing an integrated hydrodynamic-biokinetic model for an orbal bioreactor in a full-scale WWTP.

With regards to the flow field behaviours, 3D simulation can provide more information to the designers with a better understanding of how the bioreactor geometry affects flow field within the WWTP tanks [16]. Using CFD, Patziger [17] presented a numerical study to optimize the inlet geometry design of primary settling tanks. As a result of this study, improving the removal efficiency, especially at high load, led to decreasing the loads at the biological treatment process and increasing biogas and energy production. Optimization of aeration in the activated sludge processes based on CFD was performed in [18].

Conventional rectangular geometry bioreactor is still used in many WWTPs. There are different bioreactor geometries used earlier without utilising design methods to select the suitable tank geometry. The most common types are rectangular, oxidation ditch and orbal configurations. Each bioreactor configuration has its own hydrodynamic performance. Since the wastewater treatment efficiency highly depends on the flow field in the bioreactor, the hydrodynamics-based design is necessary to guide the designers for a successful design. Therefore, the objective of this study is to investigate the effect of bioreactor geometry on the hydrodynamics performance of the flow field and velocity distribution with the operation of submerged impellers using the CFD approach.

## 2. Wastewater treatment of an anoxic bioreactors

The hydrodynamics design of an anoxic bioreactor tank is based on its required pollutant removal rate which is affected by flow velocity distribution inside the tank. Therefore, a brief overview of anoxic bioreactor tank feature for nutrient removal is given with hydrodynamic design considerations.

### 2.1. Biological process

The bioreactor of a biological nutrient removal (BNR) system is divided into different stages, namely anaerobic, anoxic, and aerobic zones. Provision for mixed liquor recirculation is necessary for the biological process, as illustrated in Fig. 1. Each zone in the bioreactor is designed to provide different row wastewater conditions to allow for the micro-organisms within that zone the best chance of treatment. The aerobic zone is required in BNR processes, while the anaerobic stage is necessary to accomplish phosphorus removal, and the anoxic zone is needed for nitrogen removal.

The presence of anoxic stage impacts the biomass's microbial ecology. In nitrogen removal systems, the initial anoxic zone acts as an anoxic selector to limit the growth of filamentous bacteria through metabolic selection.

In addition to the differences between the aerobic and anaerobic reactors in terms of biological treatment, there are considerable differences in their hydrodynamics. Climent et al. [11] investigated the hydrodynamics of the flow inside a ditch with and without aeration and they found considerable differences due to the momentum transfer from bubbles. However, the present study focuses only on the anoxic zone which requires mixing in absence of the aeration process. Hence, the study of the hydrodynamics of aerobic reactors is out of the scope of the present study.

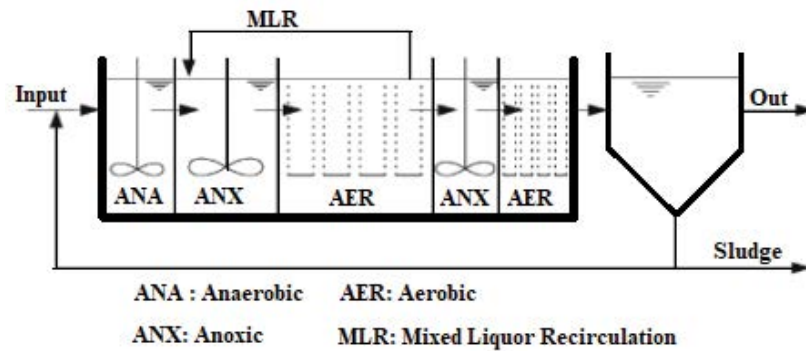


Fig. 1. Biological nutrient removal process.

## 2.2. Submerged impeller

The mixing process in the anoxic zone is important to keep the solid matter suspended in the bioreactor tank. However, the Water Environment Federation's Manual suggests that anoxic zone requires thorough mixing to maintain good contact between biomass substrates and prevent short-circuiting of flow [3]. Moreover, the mixing creates homogeneous uniform composition and temperature across the flow direction. Also, the mixer increases the heat transfer inside the bioreactor and dispersion of the fluid [3]. Additionally, the mixer can influence mass transfer and aggregation breakage of particles which increase biological reactions performance. Mechanical mixers are the most common mixers in the wastewater industry especially the propeller type, as shown in Fig. 2. The propeller mixer was selected in this study due to its good performance for wide channel plug-flow and circulation of large bioreactors.

## 2.3. Minimum flow velocity in bioreactor

Poor flow field may cause particle settlement which leads to reduction of the biological performance of bioreactor. To overcome this problem, the flow velocity inside the reactor should be maintained higher than a certain minimum velocity to avoid sedimentation of micro-organisms. Different recommendations were stated that the minimum velocities should be 0.3 m/s [19–21]. Furthermore, based on the mixer requirements and consideration that released from several mixer manufacture companies, the minimum velocity to attain sufficient suspension of activated sludge is suggested as 0.3 m/s [3]. The main criteria for analysing the result of the present study is the minimum required flow velocity being equal to 0.3 m/s and the flow range between 0.3 to 0.6 m/s.

## 2.4. Power requirement

According to Cumby [20], the required mixer power should be satisfied to maintain the minimum flow speed inside the bioreactor tank. He stated that the specific power dissipation for the system can be expressed as:

$$P_s = \frac{P_M}{V} \quad (1)$$

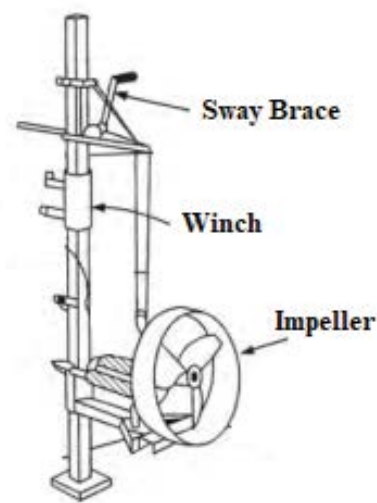


Fig. 2. Impeller mixer.

where  $P_s$  is the specific power dissipation ( $\text{kW}/\text{m}^3$ ),  $P_M$  is the power of mixers ( $\text{kW}$ ) and  $V$  is the volume of the tank ( $\text{m}^3$ ).

Tchobanoglous et al. [22] stated that the typical specific power dissipation for mechanical mixing in anoxic zones ranges from 0.008 to 0.012  $\text{kW}/\text{m}^3$ . Furthermore, this is supported by the recommendation from the Water Environment Federation which recommends that the power requirement for mixing is 0.01  $\text{kW}/\text{m}^3$  [21]. The tank volume is kept constant for all bioreactor geometries at 3,400  $\text{m}^3$ . Three impeller thrust force scenarios are considered in this study as 2800 N, 3400 N and 4000 N.

## 3. Numerical methodology

Prediction of flow behaviour inside different configurations of bioreactor tanks was numerically investigated in the present study using CFD. The numerical simulation was performed using ANSYS Fluent 18.2 software.

### 3.1. Computational geometry

The oldest bioreactor geometry is a rectangular tank and still used in many WWTPs. oxidation ditch configurations were developed as a wastewater treatment bioreactor

in the early 1960s. The orbal bioreactor is a modification of oxidation ditch system. Rectangular, oxidation ditch and orbal full-scale bioreactors have been chosen in this study. The tank geometries were selected with some considerable simplifications in order to predict and analyse the effect of bioreactor geometries on their hydrodynamics performance. The influent flow capacity was kept constant at 3,400 m<sup>3</sup> for all bioreactors. The same water depth and channel width parameters were kept constant at 2.5 and 18 m, respectively for all tested tanks. The features of the selected bioreactor geometries are illustrated in Fig. 3. All geometrical dimensions are dimensionalized based on the thruster diameter (1 m).

### 3.2. Mesh grid

Grid meshes were generated in 3D domains using ANSYS Meshing 18.2. Structured meshes were used for all different bioreactor configurations. Two different mesh configurations were examined in this study, namely, course and fine meshes. The grid size information is summarized in Table 1 and grid meshes structure are shown in Fig. 4. The calculation time is approximately one day for each steady-state calculation case. Intel (R) core (TM) i9-9880H computer was used with 2.30 GHz base frequency and 32 GB RAM. It can be noticed that no significant changes occur in solver residual results between coarse and fine meshes. Therefore, all study cases are investigated by using course mesh.

### 3.3. Simulation of submerged impeller

The main purpose of the impeller is to generate an axial flow velocity in order to drive the fluid inside the reactor. All presented bioreactors are driven by four submerged impellers and each impeller has a diameter of 1 m. A fan model was adopted for simulation of the submerged impeller in this study, in which each impeller was assumed as a thin cylinder and the pressure difference across the impeller was calculated based on the area of the disc and total power required [Eq. (1)] as shown in Fig. 5. The same impeller modelling technique was followed by Weidong et al. [8]. The total thrust requirements were estimated for three scenarios at 2800 N, 3400N to 4000 N for each fan. The total fans thrust

is estimated for each thrust scenario to be equivalent to a pressure jump as

$$T = \Delta P \cdot A \quad (2)$$

where  $A$  is the disc area,  $\Delta P$  is the pressure difference and  $T$  is the thrust force of the submerged impeller.

### 3.4. Boundary conditions

The model boundaries of each tank configuration were named in regard to their setting, as illustrated in Fig. 6. The flow phase was selected as a pure water at 20°C with a density of 998.2 kg/m<sup>3</sup>.

The no-slip boundary condition was assigned for all walls of the tank while the tank top was defined as symmetric boundary condition. The fan model was used for the submerged impeller and the surface of the impeller disc was defined as a fan boundary conditions representing the axial pressure difference.

### 3.5. Setting up the solver

The fluid flow inside three different full-scale wastewater bioreactor tanks was modelled as a single-phase flow using the commercial CFD software ANSYS-Fluent in the steady mode. The 3D version of ANSYS-Fluent was utilized. The coupled pressure-based algorithm was

Table 1  
Model grid features

Tank shape		Number of elements	Number of nodes
Orbal	Course	1440000	1454100
	Fine	7689600	7764894
Rectangle	Course	2400000	2432200
	Fine	7680000	7783040
Ditch	Course	2880000	2918640
	Fine	7728000	7831684

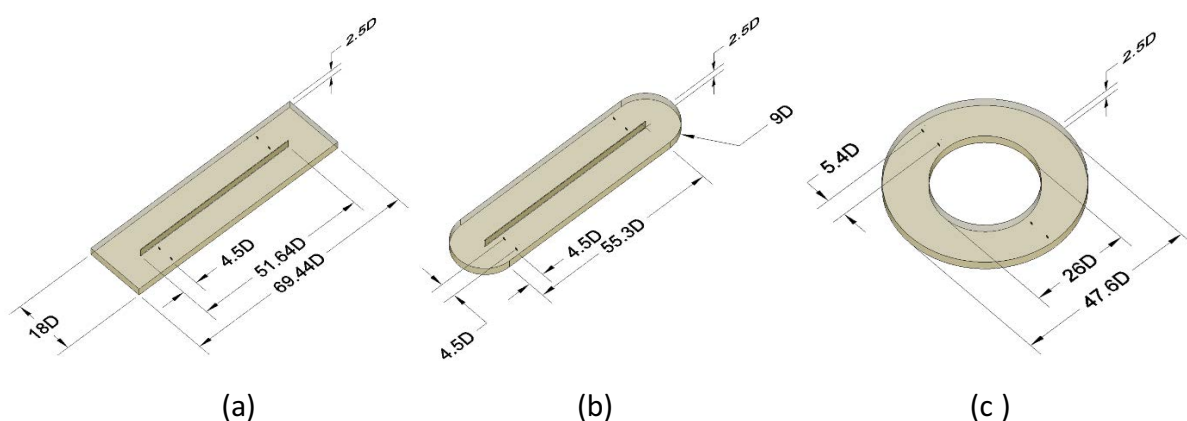


Fig. 3. The features of the three bioreactor geometries: (a) rectangular, (b) oxidation ditch, and (c) orbal.

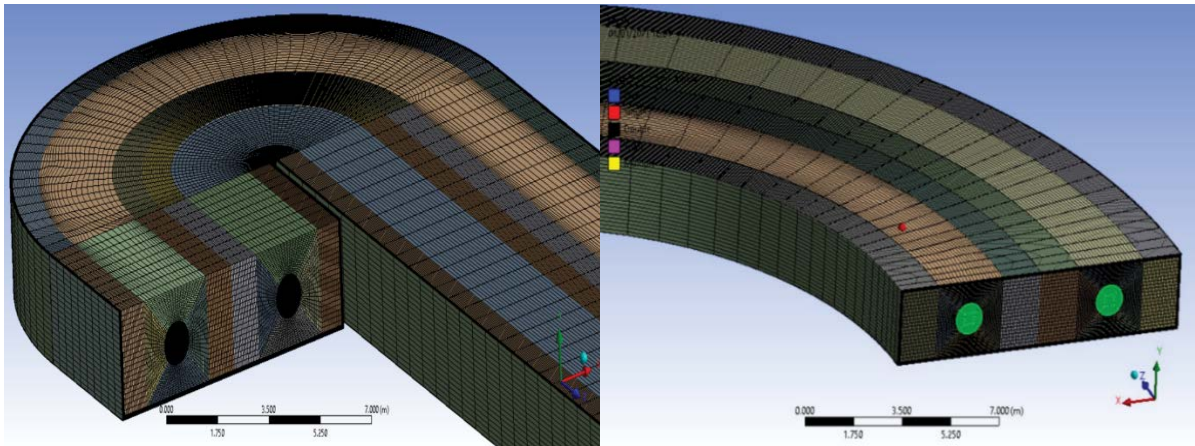


Fig. 4. Grid meshes for bioreactor geometries.

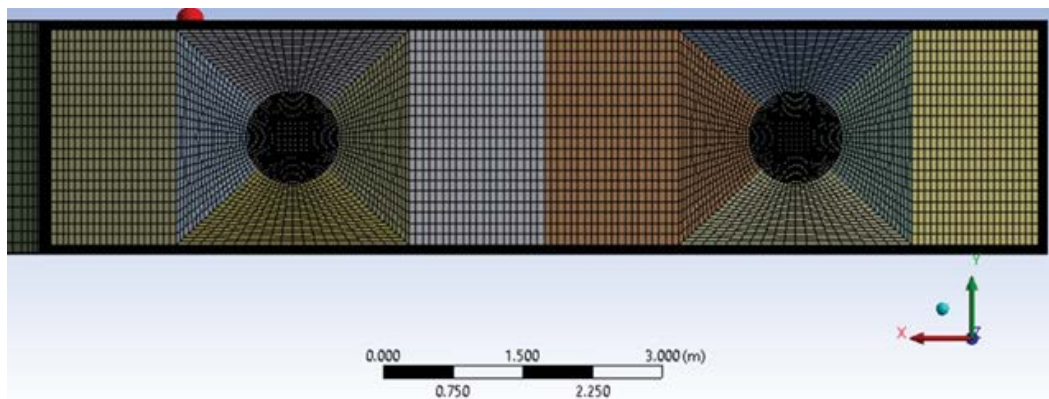


Fig. 5. Meshing of fan model.

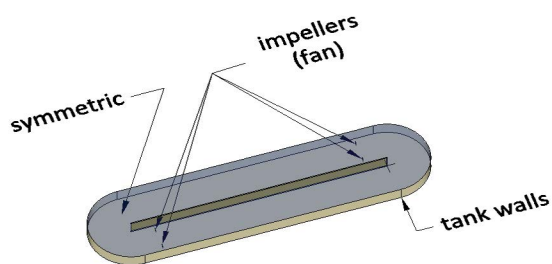


Fig. 6. Boundary conditions.

implemented for its accuracy and fast convergence. The second-order special discretization was implemented in order to improve the solution accuracy. Furthermore, the standard two-equation SST  $k-\epsilon$  model was considered for turbulence modelling.

### 3.6. Validation of the CFD model

CFD has been found as a powerful tool for accurate simulation in a wide range of fluid flow problems. However,

it is essential to validate the current CFD model by comparing its predictions against the available experimental data. For this purpose, the experimental data presented by Climent et al. [11] for full-scale ditch without aeration is utilised. Fig. 7 illustrates the configuration of the full-scale ditch and the locations of measurements. Fig. 8 presents a comparison between the CFD predictions of velocity and the corresponding experimental data at two different locations. It is observed that the CFD predictions have a good agreement with the experimental data.

### 3.7. Simulation matrix

Three bioreactor geometries were modelled at three different impeller thrust scenarios. The results are analysed at two main horizontal plan (0.1 and 0.5  $y/H$ ) where  $y$  is the horizontal plan position and  $H$  is the bioreactor water depth. Other three cross-sectional vertical plans are analysed in order to evaluate the flow velocity distribution in the vertical direction. The flow velocities were evaluated at three different test locations (a, b and c) inside the tank at different water depth heights. The distance between each vertical plan is equal to  $20D$ . The distance between location (a) and impellers is about  $20D$ , and

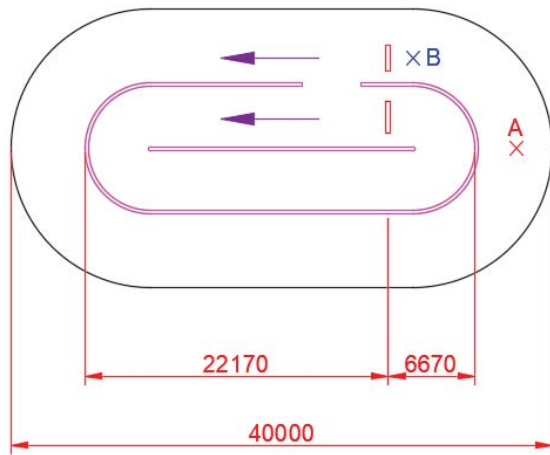


Fig. 7. Illustration of the full-scale ditch and the locations of measurements (dimensions are in mm).

between locations (a) and (b) is also  $20D$ , and location (c) is placed parallel to the internal wall, as shown in Fig. 9. In each location, the measurement data were collected at the centre of the channel. Moreover, two other measurements were collected at  $2D$  distance from the left side and right side of the channel centre. The CFD simulation matrix can be summarized as shown in Table 2.

#### 4. Results and discussions

The following section presents various simulation results from CFD model of the three bioreactor tank configurations. The numerical results from the 3D model can describe the flow field within the anoxic bioreactor and distinguish the high and low velocities which can provide a better understanding of how the geometry of the bioreactor can influence the flow field behaviour. The main criteria for analysing the result is the flow velocity distribution through each tank configuration.

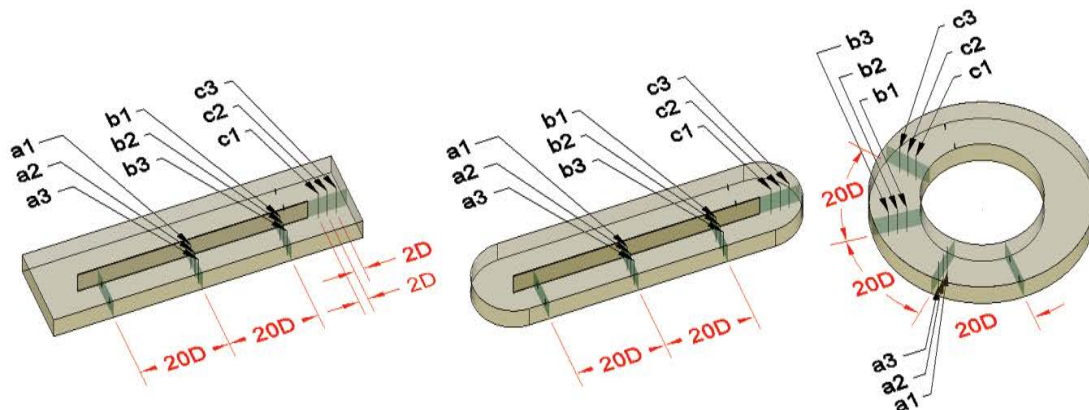


Fig. 9. Distribution of measurement locations.

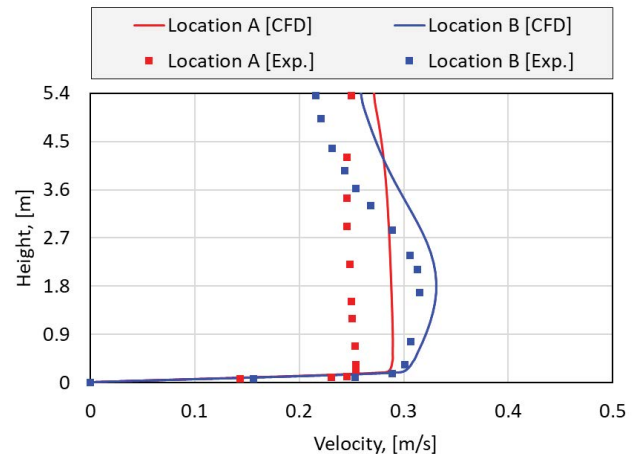


Fig. 8. A comparison between the CFD predictions and the detailed experimental data for the water velocity at two different locations.

#### 4.1. Rectangular tank configuration

Simulated velocity contour results of the rectangular tank under three different impeller thrust forces (2800 N, 3400 N and 4000 N) are shown in Fig. 10. Fig. 10a–c represent the top view of flow velocity contours on a horizontal plan at  $0.5 y/H$  (same level of impeller centre). While Figs. 10d–g represent the top view at  $0.1 y/H$  near the tank bottom. Generally, increasing impeller thrust is a procedure to avoid sludge sedimentation inside the reactor when the flow velocity decreases lower than the minimum required flow velocity (0.3 m/s). When the thrust was increased from 2800 N to 4000 N, flow velocity near the external walls was obviously improved and velocity became much higher than required. The flow velocities around the corners and internal wall were also improved but still have the same lower velocities than required.

In order to analyse the mixing quality inside the bioreactor, three iso-surfaces were plotted in three different colours.

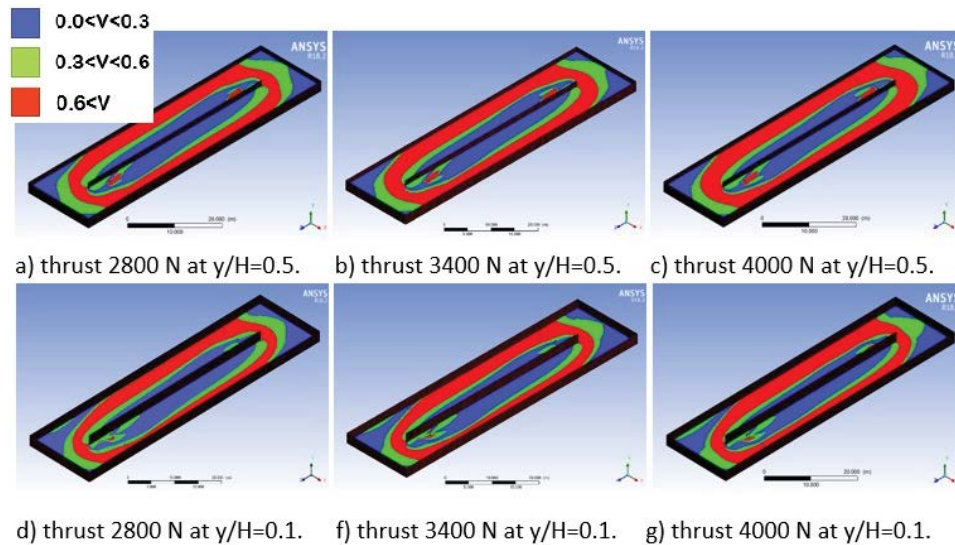


Fig. 10. Velocity contour of the rectangular bioreactor in the horizontal section at different height and different impeller thrust forces.

From 0 to 0.3 m/s range is the blue region, for 0.3–0.6 m/s range is the green region and over 0.6 m/s is the red region. In general, water circulation with a velocity above 0.6 m/s almost covers most of bioreactor regions, but areas with a lower water velocity (under 0.3 m/s) exist at tank corners and near intermediate wall due to local recirculation patterns. It can be observed that there are no significant changes in the velocity distributions of the flow field when the thrust increases from 2800 N to 4000 N.

Simulated streamline velocity profile of the rectangular tank under impeller thrust equal to 2800 N is shown in Fig. 11. The simulation result indicates that a heterogeneous flow pattern was developed within the rectangular bioreactor especially at the tank corners and beside the intermediate wall. It can be observed also that the right impeller generates uniform forward flow pattern, while the lift impeller thrust is blocked by eddies generated in this area.

Fig. 12 presents the velocity profile for nine locations inside the bioreactor as described in simulation matrix Table 2. The minimum required flow velocity which recommended in section 2.3 is plotted in yellow dashed vertical line at 0.3 m/s. Measured group (a) which located near to intermediate wall show flow velocity lower than the minimum required in two locations, while the remain groups measurements (b and c) exceed the recommended velocity limit as shown in Fig. 12. The flow velocity measured in group (c), which located near the external wall, exceed the required velocity with about four time.

#### 4.2. Oxidation ditch configuration

Simulated velocity contour results of the oxidation ditch tank under three different impeller thrust forces (2800 N, 3400 N and 4000 N) are shown in Fig. 13. Fig. 13a–c represent the top view of flow velocity contours on a horizontal plan at 0.5  $y/H$  (same level of impeller centre). While Fig. 13d–g represent the top view at 0.1  $y/H$  near the tank

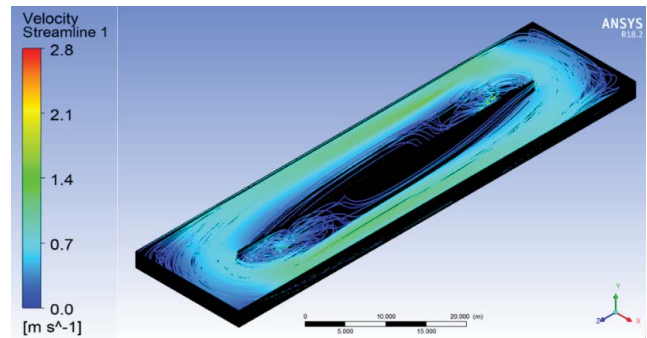


Fig. 11. Streamline velocity in the horizontal section of the rectangular tank at impeller thrust of 2800 N.

bottom. Similar to rectangular tank results, the water circulation with a velocity of above 0.6 m/s almost covers most of bioreactor regions, but areas with a lower water velocity (under 0.3 m/s) exist near intermediate wall due to local recirculation patterns. While the contribution of rounded corners to flow circulation prevents dead flow velocity spots near corners with respect to rectangular geometry.

Simulated streamline velocity profile of the oxidation ditch tank under impeller thrust is equal to 2800 N as shown in Fig. 14. The simulation results indicate that a heterogeneous flow pattern was developed within the oxidation ditch bioreactor especially beside the intermediate wall. It can be observed also that the right impeller generates uniform forward flow pattern, while the lift impeller thrust is blocked by eddies generated in this area.

Fig. 15 presents the velocity profile for nine locations inside the oxidation ditch bioreactor as described in simulation matrix Table 2. Same observation of rectangular bioreactor was also observed for the oxidation ditch tank. Group measurement (a) shows that flow velocity is lower than the

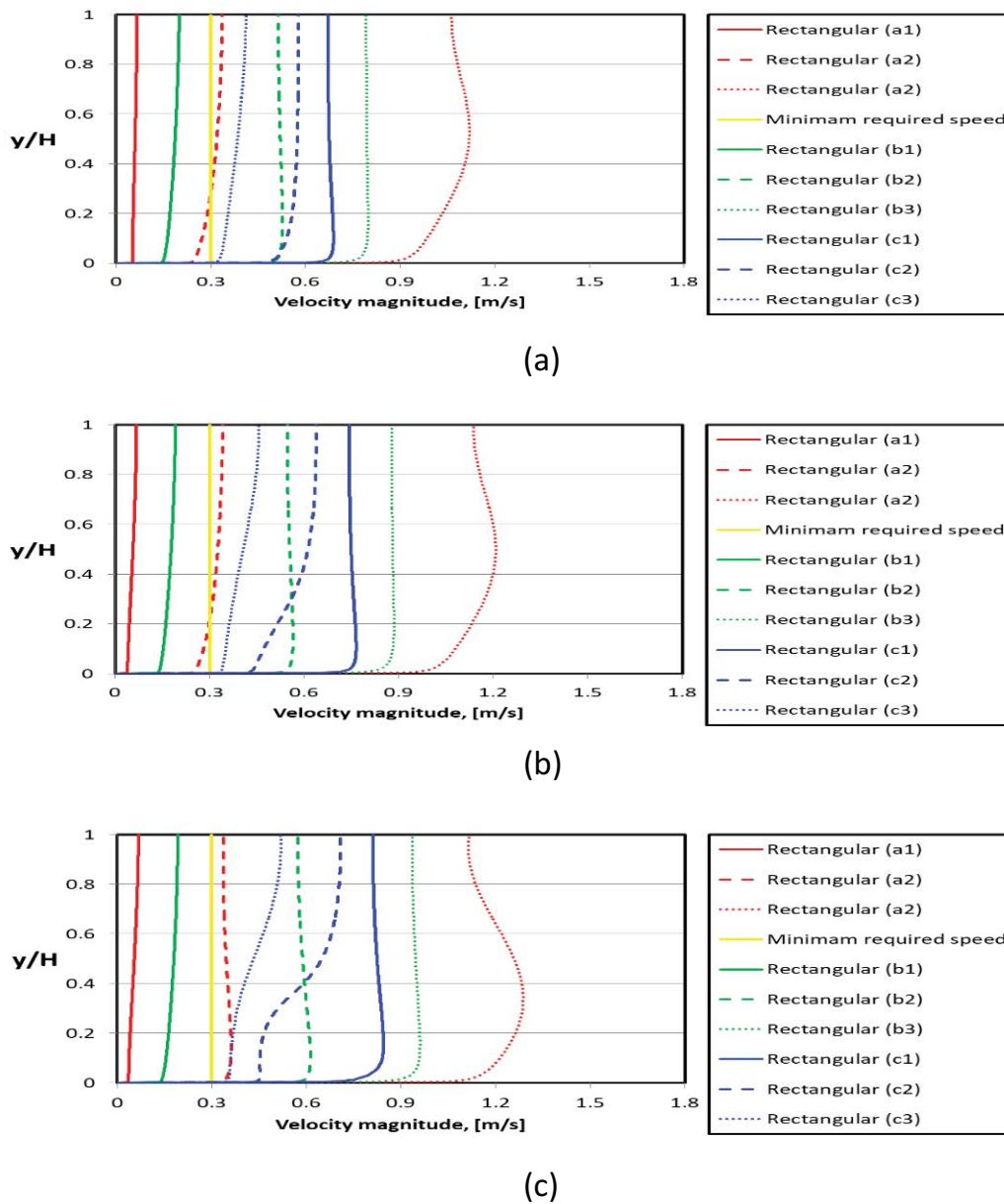


Fig. 12. Vertical flow velocity profile for a rectangular bioreactor at nine different locations for the three thrust scenarios: (a) Thrust of 2800 N, (b) Thrust of 3400 N, and (c) Thrust of 4000 N.

minimum required in two locations, while the remaining group measurements (b and c) exceed the recommended velocity limit.

#### 4.3. Orbital tank configuration

Simulated velocity contour results of the orbital tank under three different impeller thrust forces (2800 N, 3400 N and 4000 N) are shown in Fig. 16. Fig. 16a–c represent the top view of flow velocity contours on a horizontal plan at 0.5  $y/H$  (same level of impeller centre). While Fig. 16d–g represent the top view at 0.1  $y/H$  near the tank bottom. The simulation results incorporating the submerged impeller at 2800 N thrust force indicate that majority of the velocities

across the bioreactor areas are above the required limit. The water circulation with a velocity above 0.3 m/s almost covers most of bioreactor regions at impeller thrust being equal to 2800 N, but area with a lower water velocity (under 0.3 m/s) exists only between the impellers.

It can be observed that when the thrust increases, the flow velocity increases more than the required flow velocity. The flow velocity almost homogenises over the most of tank area except near the thrust and internal wall.

The streamline velocity contour illustrates the flow path and the corresponding velocities through the orbital bioreactor under impeller thrust of 2800 N as shown in Fig. 17. The simulation results indicate that a homogenised flow pattern is developed within the orbital bioreactor. It can also be

Table 2  
CFD simulation matrix

Case No.	Bioreactor geometry	y/H	Impeller thrust	Cross location	
1	Rectangular	0.1	2800 N	For each bioreactor at each water level (y/H) at each impeller thrust, three horizontal locations a, b and c and at each location 3 lateral measurements	
2			3400 N		
3			4000 N		
4			0.5		2800 N
5					3400 N
6					4000 N
7	Oxidation ditch	0.1	2800 N	- a1, a2, a3 (near the internal wall); - b1, b2, b3 (middle of the tank); - c1, c2, c3 (near the external wall).	
8			3400 N		
9			4000 N		
10			0.5		2800 N
11					3400 N
12					4000 N
13	Orbal	0.1	2800 N		
14			3400 N		
15			4000 N		
16			0.5		2800 N
17					3400 N
18					4000 N

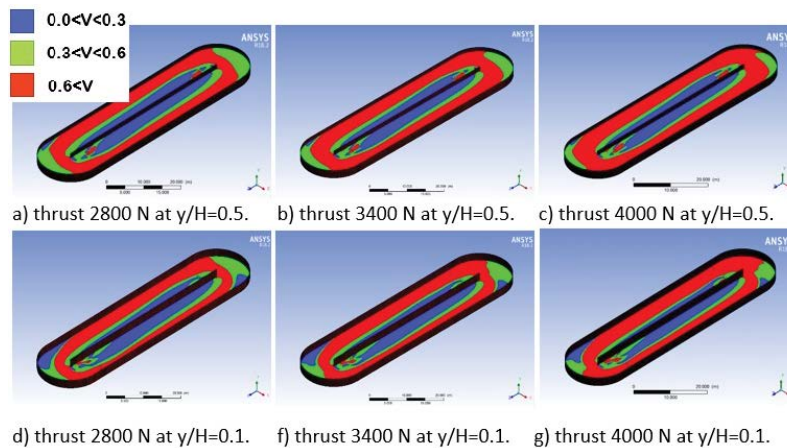


Fig. 13. Velocity contour of the oxidation ditch bioreactor in the horizontal section at different height and different impeller thrust forces.

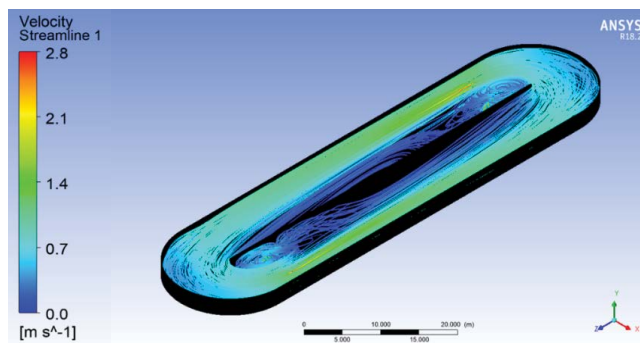


Fig. 14. Streamline velocity in the horizontal section of the oxidation ditch tank at impeller thrust of 2800 N.

observed that no local recirculation is generated and the flow is uniform.

Fig. 18 presents the velocity profile for nine locations inside the orbal bioreactor. It can be noticed that all measured group (a, b and c) show flow velocity higher than the minimum required velocity. It can also be observed that there is no significant change in the velocity profile for all locations which gives an indication that the velocity is homogeneous and uniform across the bioreactor.

#### 4.4. Comparison of velocity profile under different operational conditions

Fig. 19a–c present vertical cross section iso-surface contours throughout each tank geometry at three different

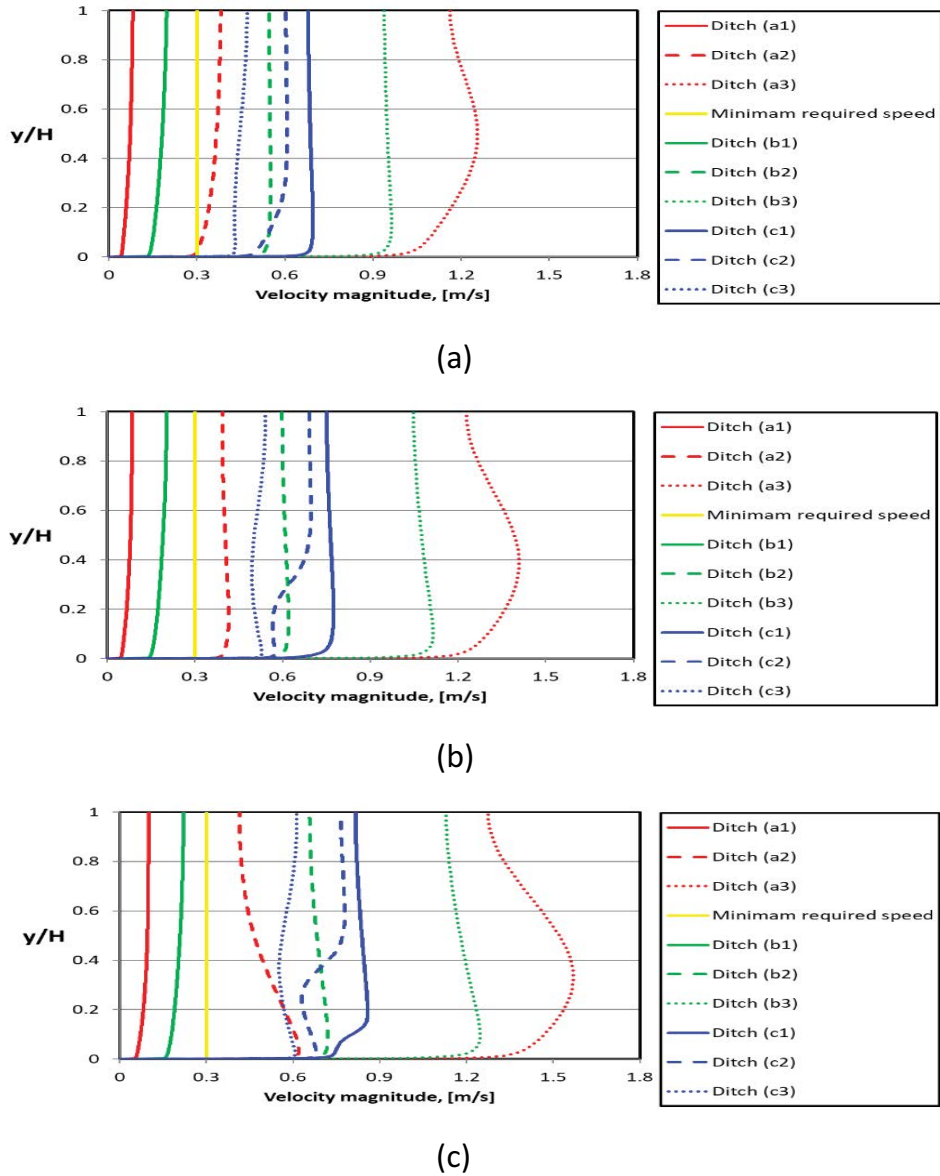


Fig. 15. Vertical flow velocity profile for oxidation ditch bioreactor at nine different locations for the three thrust scenarios: (a) Thrust of 2800 N, (b) Thrust of 3400 N, and (c) Thrust of 4000 N.

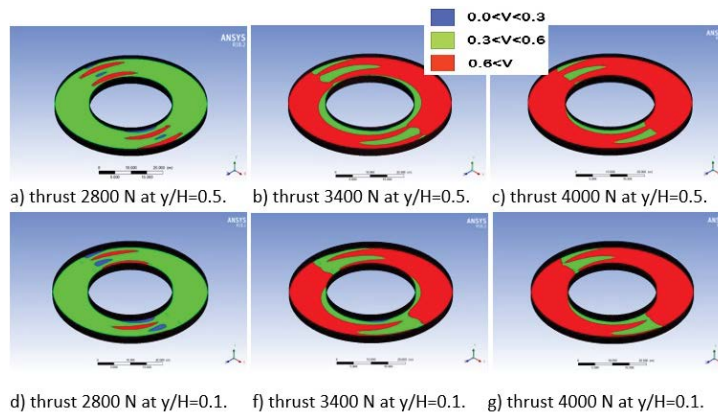


Fig. 16. Velocity contour of the orbital bioreactor in the horizontal section at different height and different impeller thrust forces.

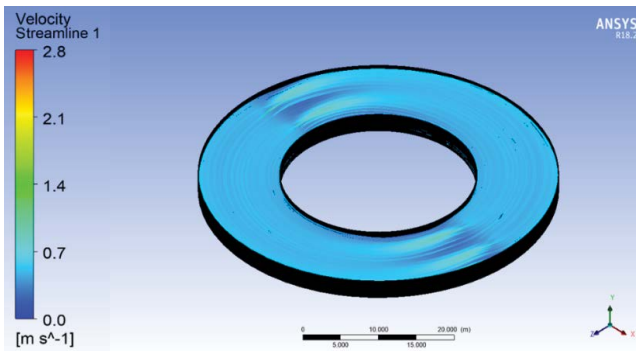


Fig. 17. Streamline velocity in the horizontal section of the orbital tank at impeller thrust of 2800 N.

impeller thrust force scenarios. Fig. 19a indicates that the flow velocity inside the orbital tank is totally homogeneous in the range of 0.3–0.6 m/s. While in oxidation ditch and rectangular the flow velocity is heterogeneous and the flow velocity drops below the minimum required velocity beside the intermediate wall and at corners. This flow velocity observation increases near tank bottom rather than the middle and at tank surface. It can be concluded from Fig. 19a that the selected impellers are capable to generate the required thrust to achieve the minimum required flow velocity in the orbital tank. This observation is the same when the impeller thrust is increased to 3400 N and 4000 N as shown in Fig. 16b and c, respectively. It should be noted that the flow velocity exceeds 0.6 m/s in large regions inside the orbital tank.

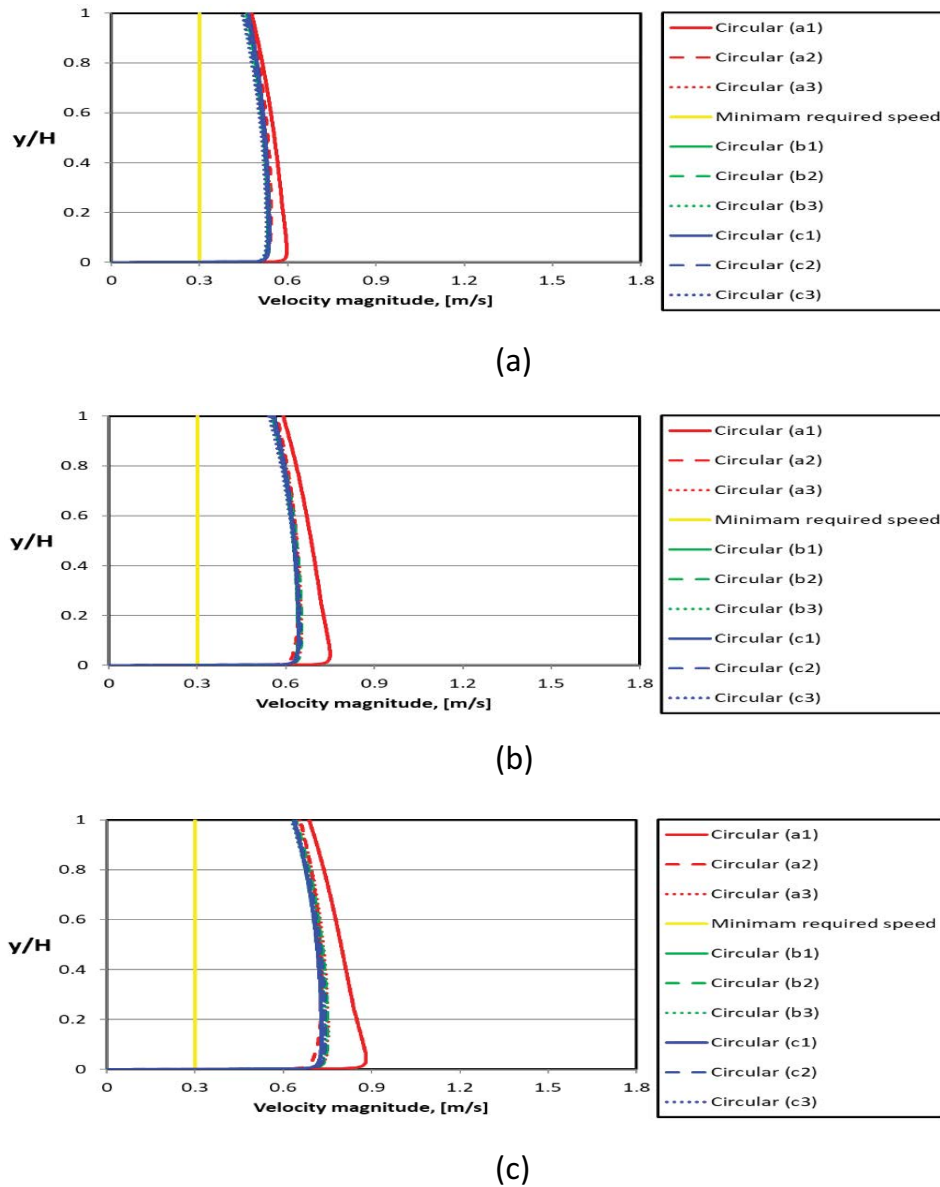


Fig. 18. Vertical flow velocity profile for orbital bioreactor at nine different locations for the three thrust scenarios: (a) Thrust of 2800 N, (b) Thrust of 3400 N, and (c) Thrust of 4000 N.

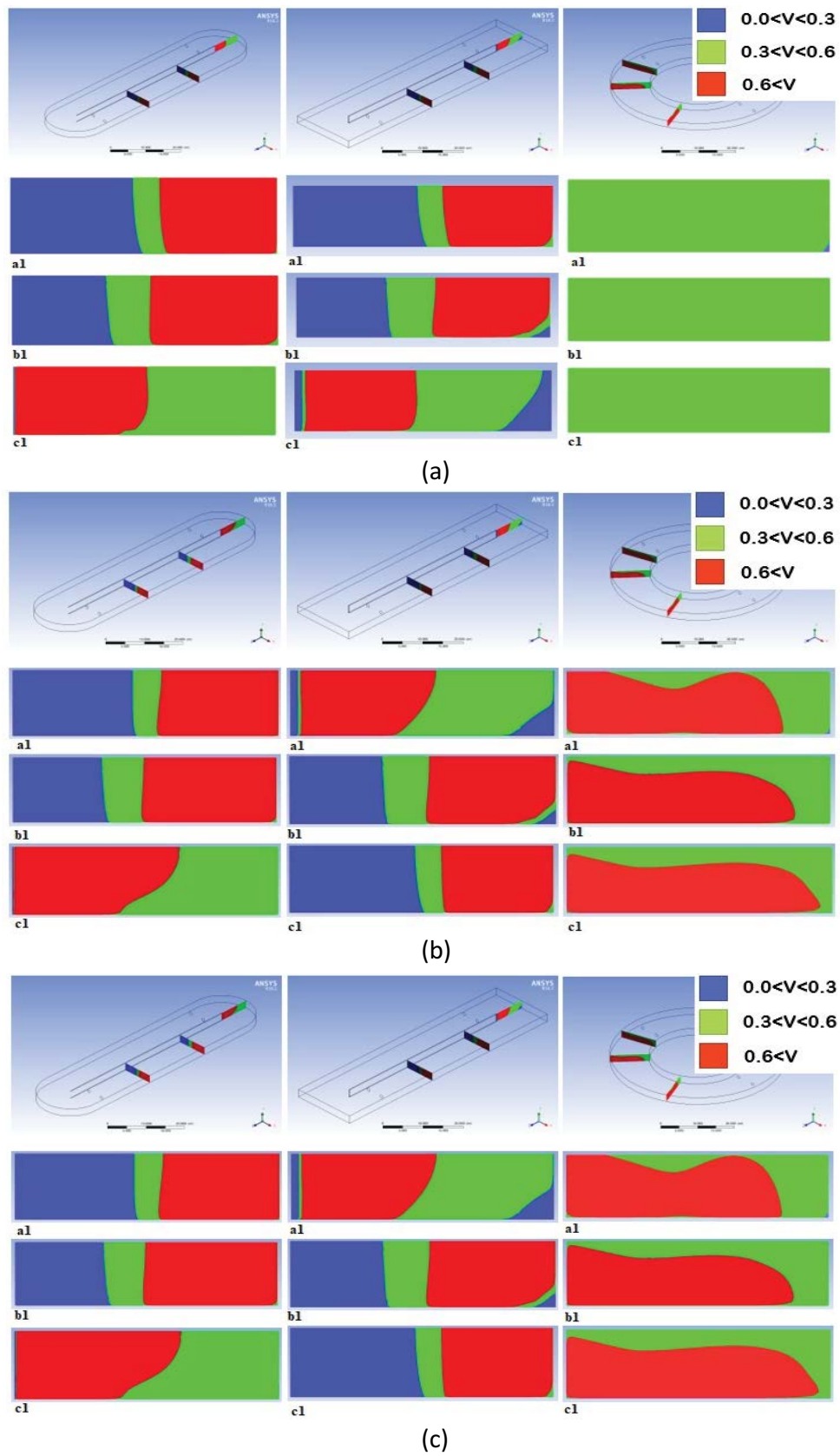
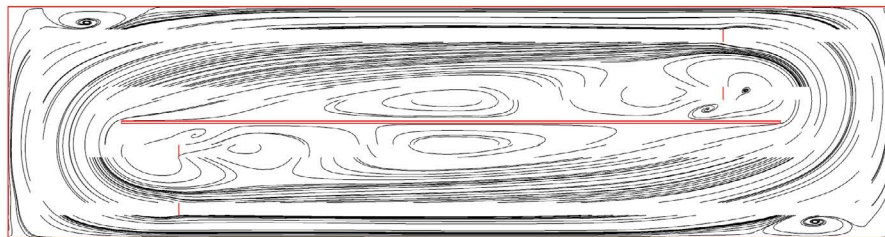


Fig. 19. Flow velocity contour of different bioreactor geometries in the vertical cross section at different impeller thrust forces: (a) Thrust of 2800 N, (b) Thrust of 3400 N, and (c) Thrust of 4000 N.

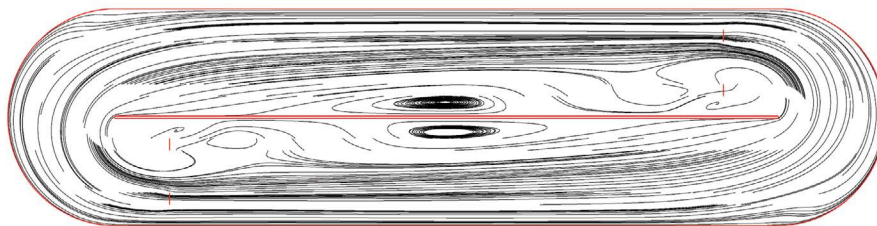
In case of obal bioreactor, the flow streamline pattern is homogeneous and uniform across the tank as shown in Fig. 20c. Whereas in case of rectangular and oxidation ditch bioreactors, the water circulation almost covers most of bioreactor regions near external tank wall and while the area near intermediate wall suffers from eddies due to local recirculation patterns. Local recirculation patterns also appear in rectangular tank at corners, while the contribution of rounded corners of oxidation tank prevent this phenomenon.

The concept of flow uniformity has been successfully used to evaluate and optimize the flow quality at working

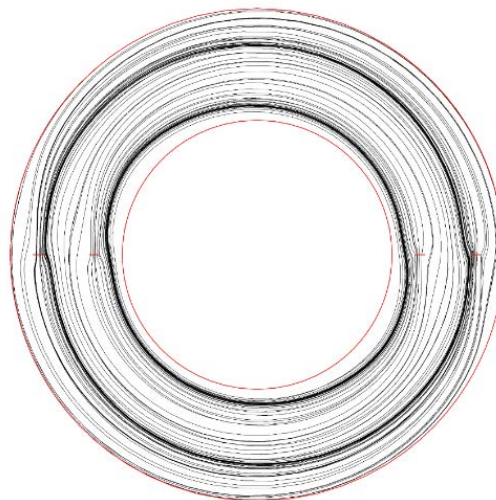
sections [23]. The flow uniformity is defined as the ratio between the average velocity and the maximum velocity at a certain cross-section. When the average velocity becomes close to the maximum velocity, the flow uniformity increases. The flow uniformity for inviscid undisturbed flow is unity. However, the flow uniformity in bioreactor tanks is less than unity due to the boundary layer effects and the possible eddies and separation. Fig. 21 illustrates the flow uniformity for the three selected cross-sections, namely (a), (b), and (c), for the three tank geometries at different impeller thrusts. It is observed that the value of the thrust has a minimal effect on the flow uniformity.



(a)



(b)



(c)

Fig. 20. Streamline contours for three bioreactor geometries at impeller thrust of 2800 N: (a) rectangular bioreactor, (b) oxidation ditch bioreactor, and (c) orbital bioreactor.

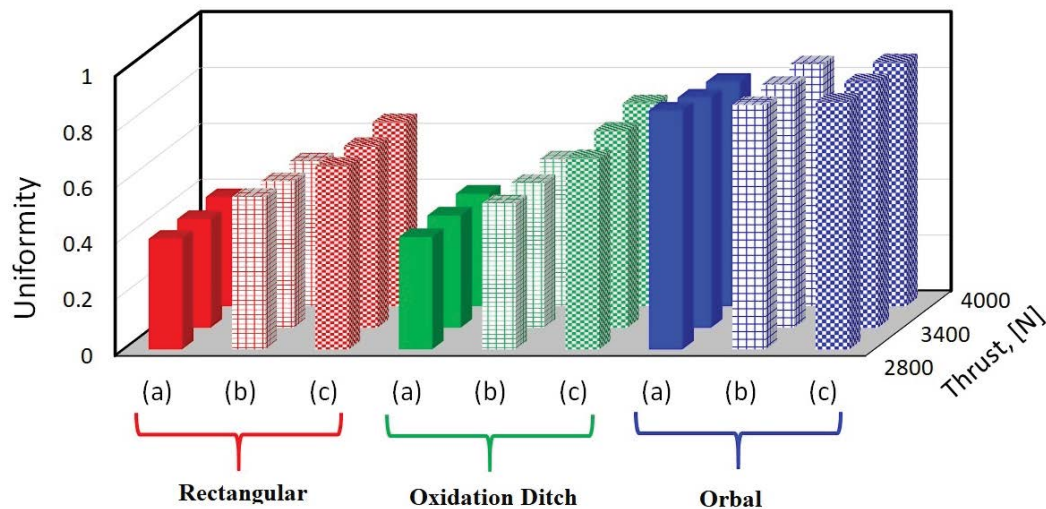


Fig. 21. The flow uniformity for cross-sections (a), (b), and (c) for the three tank geometries at different impeller thrusts

However, the location of the test cross-section has a considerable influence on the flow uniformity, especially for the rectangular and ditch tanks. In contrast with the rectangular and ditch tanks, it is observed that the orbal configuration achieves a very good flow uniformity at the three tested cross-sections for all the tested impeller thrusts.

## 5. Conclusions

The hydrodynamics design of anoxic bioreactor tank has significant impact on energy consumption and biological performance of wastewater treatment plants. A computational fluid dynamic model of different bioreactor configurations was numerically investigated by considering flow field and minimum velocity parameter in order to investigate the effect of bioreactor geometry on the hydrodynamic performance of the flow field. The present model was capable of predicting flow pattern and velocity distribution with operation of submerged impellers. Performance demonstration and comparison of three different impeller thrust forces were carried out in three different full-scale bioreactor configurations. A fan model was designed to simulate the submerged impellers. The results show that the selected impellers are capable to generate the required thrust to achieve the minimum required flow velocity in the orbal tank and the flow pattern is homogeneous and uniform across the tank. Whereas rectangular and oxidation ditch geometries suffer from local recirculation patterns near the internal wall and corners affecting their flow field. Based on comparison of results and analyses, it is observed that the magnitude of the thrust has a minimal effect on the flow uniformity within the modelled bioreactors. However, the location of the test cross-section has a considerable influence on the flow uniformity, especially for the rectangular and ditch tanks. In contrast with the rectangular and ditch tanks, it is observed that the orbal configuration achieves a very good flow uniformity for the three tested cross-sections for all the tested impeller thrusts.

## Acknowledgments

This work was supported by a Institutional Links grant, ID 527426826, under the Egypt-Newton-Mosharafa Fund partnership. The grant is funded by the UK Department for Business, Energy and Industrial Strategy and Science, Technology and Innovation Funding Authority (STIFA) - project NO. 42717 (An Integrated Smart System of Ultrafiltration, Photocatalysis, Thermal Desalination for Wastewater Treatment) and delivered by the British Council.

## References

- [1] T. Höhne, T. Mamedov, CFD simulation of aeration and mixing processes in a full-scale oxidation ditch, *Energies*, 13 (2020) 1633, doi: 10.3390/en13071633.
- [2] Y. Fayolle, C. Arnaud, G. Sylvie, R. Michel, H. Alain, Oxygen transfer prediction in aeration tanks using CFD, *Chem. Eng. Sci.*, 62 (2007) 7163–7171.
- [3] M. Brannock, Computational Fluid Dynamics Tools for the Design of Mixed Anoxic Wastewater Treatment Vessels, 2003. Available at: <http://espace.library.uq.edu.au/view/UQ:106525> (accessed on 20 March 2016).
- [4] Y. Yang, J. Yang, J. Zuo, Y. Li, S. He, X. Yang, K. Zhang, Study on low operating conditions of a full-scale oxidation ditch for optimization of energy consumption and effluent quality by using CFD model, *Water Res.*, 45 (2011) 3439–3452.
- [5] C. Knatz, S. Rafferty, A. Delescinskis, Optimization of water treatment plant flow distribution with CFD modeling of an influent channel, *Water Qual. Res. J. Can.*, 50 (2015) 72–82.
- [6] S. Rigopoulos, A. Jones, A hybrid CFD-reaction engineering framework for multiphase reactor modelling: basic concept and application to bubble column reactors, *Chem. Eng. Sci.*, 58 (2003) 3077–3089.
- [7] A. Krychowska, M. Kordas, M. Konopacki, B. Grygorcewicz, D. Musik, K. Wójcik, M. Jedrzejczak-Silicka, R. Rakoczy, Mathematical modeling of hydrodynamics in bioreactor by means of CFD-based compartment model, *Processes*, 8 (2020) 1301, doi: 10.3390/pr8101301.
- [8] W. Huang, K. Li, G. Wang, Y. Wang, Computational fluid dynamics simulation of flows in an oxidation ditch driven by a new surface aerator, *Environ. Eng. Sci.*, 30 (2013) 663–671.
- [9] Y. Qiu, C. Zhang, B. Li, J. Li, X. Zhang, Y. Liu, P. Liang, X. Huang, Optimal surface aeration control in full-scale oxidation ditches

- through energy consumption analysis, *Water*, 10 (2018) 945, doi: 10.3390/w10070945.
- [10] A.M. Karpinska, M.M. Dias, R.A.R. Boaventura, R.J. Santos, Modeling of the hydrodynamics and energy expenditure of oxidation ditch aerated with hydrojets using CFD codes, *Water Qual. Res. J. Can.*, 50 (2015) 83–94.
- [11] J. Climent, R. Martínez-Cuenca, P. Carratalà, M.J. González-Ortega, M. Abellán, G. Monrós, S. Chiva, A comprehensive hydrodynamic analysis of a full-scale oxidation ditch using population balance modelling in CFD simulation, *Chem. Eng. J.*, 374 (2019) 760–775.
- [12] L. Machado, D.M. Koerich, S. Varela, D. Giustina, The use of CFD in design and optimization of wastewater treatment units: a review, *Organic Waste*, (2017).
- [13] T. Höhne, T. Mamedov, CFD simulation of aeration and mixing processes in a full-scale oxidation ditch, *Energies*, 13 (2020) 1633, doi: 10.3390/en13071633.
- [14] X. Guo, X. Zhou, Q. Chen, J. Liu, Flow field and dissolved oxygen distributions in the outer channel of the orbital oxidation ditch by monitor and CFD simulation, *J. Environ. Sci.*, 25 (2013) 645–651.
- [15] U. Rehman, W. Audenaert, Y. Amerlinck, T. Maere, M. Arnaldos, I. Nopens, How well-mixed is well mixed? Hydrodynamic-biokinetic model integration in an aerated tank of a full-scale water resource recovery facility, *Water Sci. Technol.*, 76 (2017) 1950–1965.
- [16] H. Xie, J. Yang, Y. Hu, H. Zhang, Y. Yang, K. Zhang, X. Zhu, Y. Li, C. Yang, Simulation of flow field and sludge settling in a full-scale oxidation ditch by using a two-phase CFD Model, *Chem. Eng. Sci.*, 109 (2014) 296–305.
- [17] M. Patziger, Improving wastewater treatment plant performance by applying CFD models for design and operation: selected case studies, *Water Sci. Technol.*, 84 (2021) 323–332.
- [18] Y. Fayolle, A. Cockx, S. Gillot, M. Roustan, A. Héduit, Oxygen transfer prediction in aeration tanks using CFD, *Chem. Eng. Sci.*, 62 (2007) 7163–7171.
- [19] A. Elshaw, N.M.S. Hassan, M. Masud, K. Khan, Computational fluid dynamic modelling and optimisation of wastewater treatment plant bioreactor mixer, *Energies*, 11 (2018) 3530, doi: 10.3390/en11123530.
- [20] T.R. Cumby, Slurry mixing with impellers. I. Theory and previous research, *J. Agric. Eng. Res.*, 45 (1990) 157–173.
- [21] Degremont, *Water Treatment Handbook*, Rueil-Malmaison, France, Degremont, 1991.
- [22] G. Tchobanoglous, F.L. Burton, H.D. Stensel, Metcalf and Eddy, *Wastewater Engineering: Treatment and Reuse*, Boston, McGraw-Hill, 2003.
- [23] A.S. Abdelhamed, Y.E.S. Yassen, M.M. Elsakka, Design optimization of three dimensional geometry of wind tunnel contraction, *Ain Shams Eng. J.*, 6 (2015) 281–288.